Axial dependence of optical weak measurements in the critical region

2015 J. Opt. 17 035608

(http://iopscience.iop.org/2040-8986/17/3/035608)

IOP Publishing Journal of Optics
J. Opt. 17 (2015) 035608 (10pp) doi:10.1088/2040-8978/17/3/035608

Axial dependence of optical weak measurements in the critical region

M P Araújo[1], Stefano De Leo[2,3] and Gabriel G Maia[1]

[1] Institute of Physics 'Gleb Wataghin', State University of Campinas, Brazil
[2] Department of Applied Mathematics, State University of Campinas, Brazil

E-mail: mparaujo@ifi.unicamp.br, deleo@ime.unicamp.br and ggm11@ifi.unicamp.br

Received 21 October 2014, revised 10 December 2014
Accepted for publication 22 December 2014
Published 13 February 2015

Abstract

The interference between optical beams of different polarizations plays a fundamental role in reproducing the optical analog of the electron spin weak measurement. The extraordinary point in optical weak measurements is represented by the possibility of estimating with great accuracy the Goos–Hänchen (GH) shift by measuring the distance between the peaks of the outgoing beams for two opposite rotation angles of the polarizers located before and after the dielectric block. Starting from the numerical calculation of the GH shift, which clearly shows a frequency crossover for incidence near the critical angle, we present a detailed study of the interference between s and p polarized waves in the critical region. This makes it possible to determine in which conditions axial deformations can be avoided and the GH curves reproduced. In view of a possible experimental implementation, we give the expected weak measurement curves for Gaussian lasers of different beam waist sizes propagating through borosilicate (BK7) and fused silica dielectric blocks.

Keywords: weak measurements, laser, Goos–Hänchen

(Some figures may appear in colour only in the online journal)

1. Introduction

The Goos–Hänchen [GH] shift [1–3] surely is one of the most intriguing research subjects to appear in literature in recent decades [4–12]. This shift, which is probably one of the clearest manifestations of the evanescent nature of light, represents an additional contribution to the geometrical optical path predicted by the Snell law [13, 14]. This quantum effect is still the subject of careful and broad investigation and continues to stimulate new discussion [15–22]. Of particular interest to the study presented in this paper is the GH shift frequency crossover [23]. For incidence angles θ_0 far from the critical angle, θ_c, it is well known that the GH shift is proportional to the wavelength, λ, of the optical beam [2, 4, 23, 24]. For incidence at critical angle the GH shift is amplified by a factor $\sqrt{w_0/\lambda}$, where w_0 is the beam waist. This amplification has been recently obtained analytically by using the stationary phase method [25, 26] and then confirmed by numerical calculations [23]. This frequency crossover will play a fundamental role in deriving the expected experimental curves for optical weak measurements in the critical (angle) region.

In a recent interesting experimental paper [27], by using the optical analog [28–30] of the electron spin weak measurement [31], the behavior of the GH shift curve has been reproduced in the region in which the incidence angles are far enough from the critical angle to permit some important approximations.

It is important to observe that in the optical analog of the electron spin weak measurement, polarized light plays the role of the spin $\frac{1}{2}$ particles and the laser beam replaces the coherent electron beam. Because the displacement produced by the optical system is a lateral shift rather than an angular deflection, as happens in the presence of the Stern–Gerlach magnet [31], we must consider spatial distributions instead of momentum distributions. Even though the physics is far from the same, with sufficient attention, an optical version of the electron spin weak measurement experiment can be constructed [28].

[3] Author to whom any correspondence should be addressed.

A unified linear algebra approach to dielectric reflection that recently appeared in the literature [29, 30] bases the analogy between weak values and optical beam shifts of polarized waves on the expectation value of the Artman operator. Such an operator is shown to be Hermitian for total internal reflection and non-Hermitian in the critical region [29]. For the mathematical details, we refer the reader to reference [30]. In our approach, we discuss the optical analog of the electron spin weak measurement, by analyzing, as done theoretically in reference [28] and experimentally in reference [27], the distance between the peaks of the outgoing optical beam. We recall that in the critical region, due to the breaking of symmetry [22], the peak and mean values do not necessarily coincide. In view of these comments, our discussion can be seen as a complementary work to the one which appears in reference [29, 30].

To make this introduction and the objective of our analysis clearer to the reader, we recall that in the optical analog of the quantum weak measurement [27, 28], the parameters which characterize the behavior of the distance between peaks in the experimental curves are

$$\epsilon = \epsilon_0 + \Delta\epsilon = \cos(\alpha - \beta)/\cos(\alpha + \beta), \tag{1}$$

where α and $\beta = \alpha + \frac{\pi}{2} + \gamma_0 + \Delta\gamma$ are the polarization angles of the first and second polarizer (see figure 1), and

$$\Delta y_{\rm GH} = y_{\rm GH}^{[p]} - y_{\rm GH}^{[s]}, \tag{2}$$

where $y_{\rm GH}^{[s,p]}$ are, respectively, the GH shifts for s and p polarization. For small rotation angles, i.e., $\Delta\gamma \ll 1$, and for an incoming beam with an equal mixture of polarizations, i.e., $\alpha = \pi/4$, we have

$$\epsilon_0 + \Delta\epsilon = \tan\left(\gamma_0 + \Delta\gamma\right) \approx \tan\gamma_0 + \frac{\Delta\gamma}{\cos^2\gamma_0}.$$

For incidence angles far from the critical angle, the condition

$$\Delta\epsilon \gg \Delta y_{\rm GH}/{\rm w}(z) \approx \lambda/{\rm w}(z), \tag{3}$$

where ${\rm w}(z) = {\rm w}_0\sqrt{1 + \left(\lambda z/\pi\ {\rm w}_0^2\right)^2}$, is easily satisfied and, as we shall see in detail later, the distance between the peaks of the outgoing beams for two opposite rotations in the second polarizer, i.e., $\beta_{\pm} = \frac{3}{4}\pi + \gamma_0 \pm |\Delta\gamma|$, is given by

$$\Delta Y_{\rm max} \approx \Delta y_{\rm GH}/|\Delta\epsilon|. \tag{4}$$

Consequently, for polarizer rotations which satisfy the constraint in (3), the experimental curve of $\Delta Y_{\rm max}$ reproduces the GH shift curve amplified by the factor $1/|\Delta\epsilon|$. The GH behavior and its amplification (far from the critical region) were recently confirmed in the experimental investigation presented in reference [27].

As observed at the begining of this introduction, the frequency crossover in the critical region [23] leads to

$$\Delta y_{\rm GH}^{[\rm cri]} \propto \sqrt{\lambda\ {\rm w}(z)} \gg \lambda. \tag{5}$$

This critical GH shift behavior stimulates investigation into what happens for incidence angles near the critical angle,

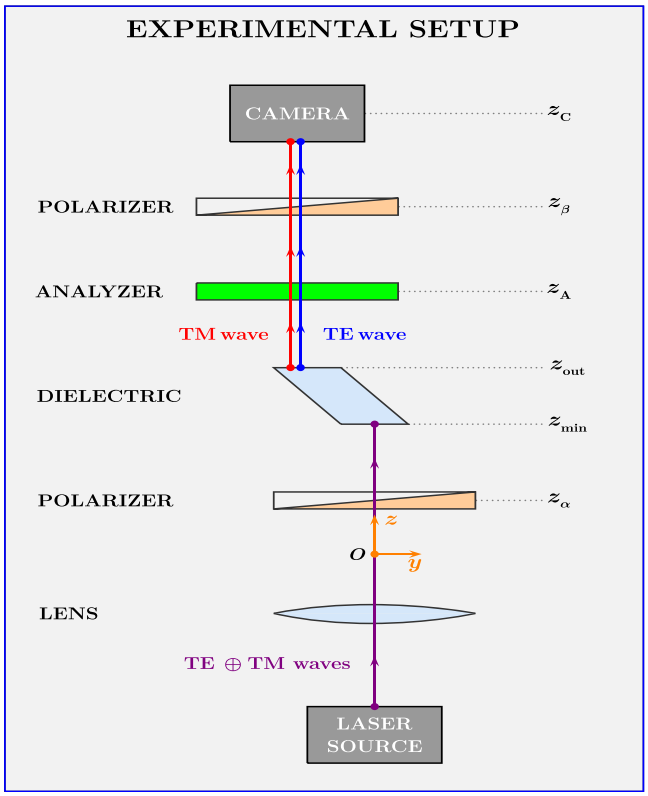

Figure 1. Experimental layout. A schematic representation of the optical weak measurement experiment for the observation of the transversal distance between the main peaks of the outgoing beams for two opposite rotations, $\pm\Delta\gamma$, of the second polarizer. The incoming beam, which, after the first polarizer ($\alpha = \pi/4$), has an equal mixture of s and p polarized waves, passes through the dielectric block ($z_{\rm in} < z < z_{\rm out}$); and then, passing through the analyzer in $z = z_{\rm A}$, loses the global $\Delta\phi_{\rm GH}$ phase. Optical weak measurements are done by changing the rotation angle in the second polarizer ($\beta = 3\pi/4 + \gamma_0 \pm |\Delta\gamma|$). The angle γ_0 is fixed to obtain, for $\Delta\gamma = 0$, an outgoing beam with two identical maxima centered at $\pm\,{\rm w}(z)/\sqrt{2}$.

where, due to the amplification $\sqrt{{\rm w}(z)/\lambda}$, the condition in (3) may no longer be valid. This should modify the shape of the experimental curves, and a new formula should be introduced to estimate the GH shift by measuring the distance between peaks, $\Delta Y_{\rm max}$. In view of a possible experimental implementation of optical weak measurements for incidence near the critical angle, we analyze the expected experimental curves for mixed polarized laser Gaussian beams with $\lambda = 633$ nm and ${\rm w}_0 = 200,\ 300$, and $500\ \mu$m propagating through BK7 and fused silica dielectric blocks.

This paper is organized as follows. In section 2, we give the transmission coefficient for the beam propagating through the dielectric structure of figure 2 and calculate the axial dependence of the GH shift for BK7 (figure 3) and fused silica (figure 4) blocks. In section 3, we introduce the idea of weak measurement in optics and analyze the effect that the polarizer and analyzer have on the s and p polarized waves of the outgoing beam. For critical incidence, new parameters have to be introduced (figure 5). The analysis of the distance between the main peaks of the outgoing beams for two

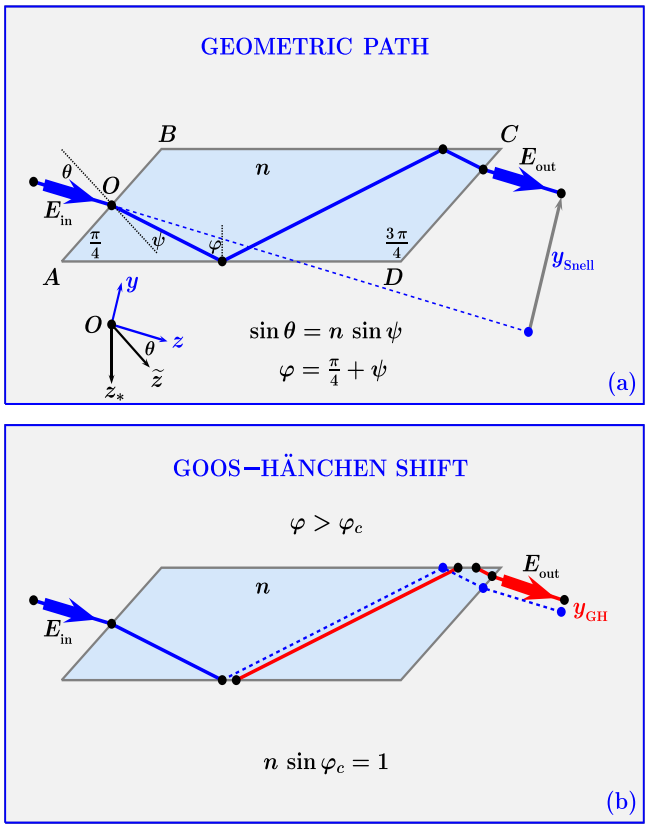

Figure 2. Geometric path and Goos–Hänchen shift. Schematic diagram of the dielectric block analyzed in this paper. (a) The geometric path predicted by the Snell law, equation (11). For $\varphi > \varphi_c$, an additional phase, coming from the Fresnel reflection coefficients at the down and up interfaces, must be considered. This phase is responsible for the addition shift, equation (13), known as the Goos–Hänchen shift and shown in (b).

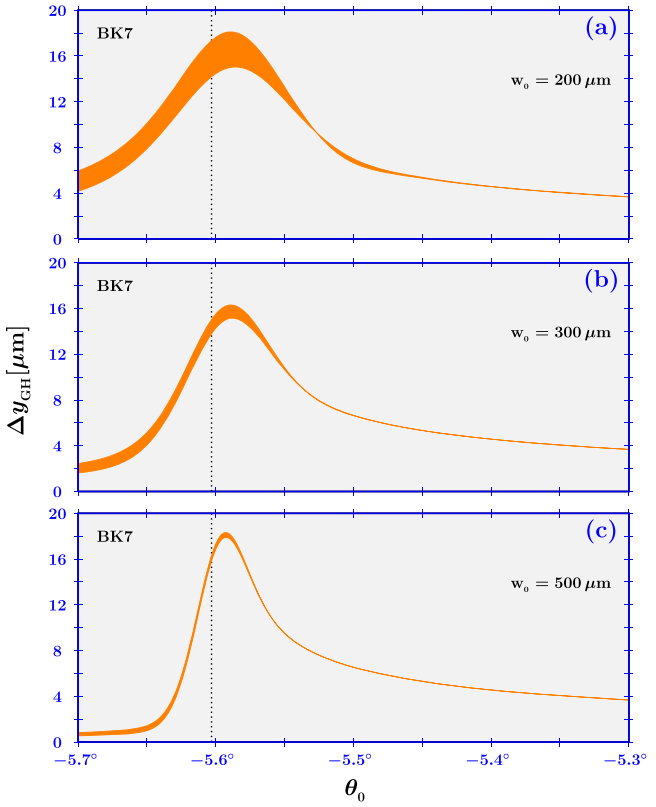

Figure 3. The GH shift curves for BK7 blocks. The numerical data for the transversal Δy_{GH} shift of laser Gaussian beams passing through a BK7 dielectric block are plotted, in the axial range 10 cm $\leqslant z \leqslant$ 15 cm for different beam waists: (a) $w_0 = 200\,\mu$m, (b) 300 μm, and (c) 500 μm. The crossover frequency at the critical angle is clear from the plots, and the axial dependence is an additional phenomenon to be considered in optical weak measurements.

opposite rotation angles of the second polarizer is presented in section 4. There a new analytical relation between the GH shift and the distance between peaks is also introduced. In this section, we also present the expected experimental curves for incoming Gaussian beams with different beam waists ($w_0 = 200$, 300, and500 μm) propagating through BK7 (figure 6) and fused silica (figure 7) dielectric blocks. The axial dependence of optical weak measurements is clear in the plots and is one of the important results of our analysis. The final section gives our conclusions and outlook.

2. The GH shift for BK7 and fused Silica blocks

To obtain the mathematical expression for the transmitted beam, $E_{out}^{[s,p]}$, propagating in the y–z plane through the dielectric block (see figures 1 and 2), let us first introduce the Gaussian wave number distribution which determines the shape of the incoming beam, $E_{in}^{[s,p]}$:

$$g(\theta-\theta_0) = \frac{k w_0}{2\sqrt{\pi}} \exp\left[-(k w_0)^2(\theta-\theta_0)^2/4\right]. \qquad (6)$$

In the electric amplitude expressions the superscript notation distinguishes between s and p polarized light. By using the paraxial approximation ($k\,w_0 \gtrsim 10$), the incoming electric field, which moves from the source laser to the left side of the dielectric block, can be represented by [13, 14]:

$$E_{in}^{[s,p]}(y,z) = E_0\, e^{ik\,z} \int_{-\pi/2}^{+\pi/2} d\theta\, g(\theta-\theta_0) \times \exp\left[i(\theta-\theta_0)k\,y - i\frac{(\theta-\theta_0)^2}{2}\,k\,z \right]$$
$$= \frac{E_0\, e^{ik\,z}}{\sqrt{1+2\,i\frac{z}{k\,w_0^2}}} \exp\left[-\frac{y^2}{w_0^2 + 2\,i\,\frac{z}{k}} \right]. \qquad (7)$$

For Gaussian lasers with a small beam waist with respect to the dimensions of the dielectric block, we can use the step technique of quantum mechanics [32–36] and give the Fresnel coefficients in terms of angles θ, ψ, and φ (see figure 2).

$$\sin\theta = n \sin\psi \quad \text{and} \quad \varphi = \psi + \frac{\pi}{4}.$$

The transmission coefficient which characterizes the outgoing

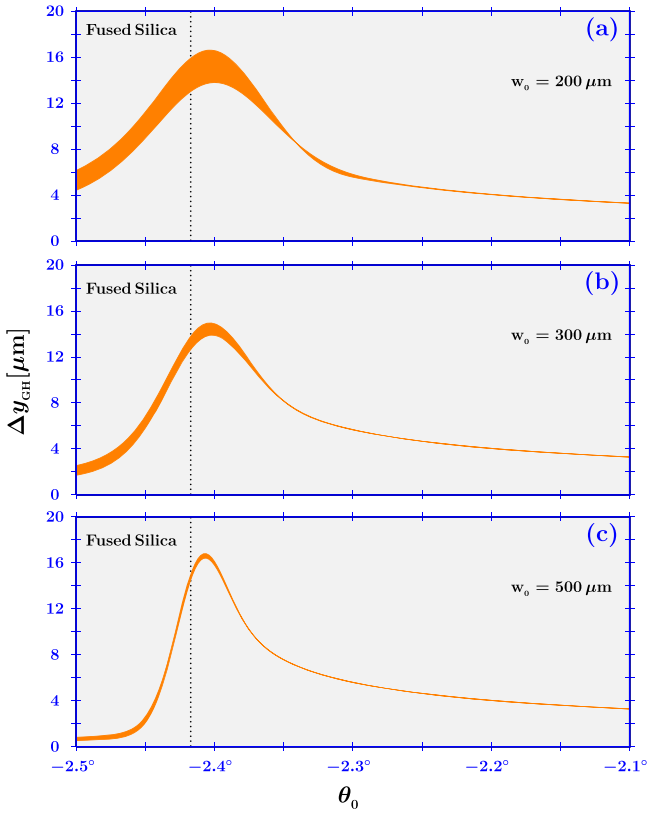

Figure 4. The GH shift curves for fused silica blocks. The numerical data for the transversal Δy_{GH} shift of laser Gaussian beams passing through a fused dielectric block are plotted in the axial range 10 cm $\leqslant z \leqslant$ 15 cm for different beam waists: (a) $w_0 = 200\ \mu$m, (b) 300 μm, and (c) 500 μm. The crossover frequency at the critical angle is clear from the plots, and the axial dependence is an additional phenomenon to be considered in optical weak measurements.

beam is obtained by the transmission through the left/right sides and the reflection between the up/down sides of the dielectric block. After simple algebraic manipulations (for more details see reference [37]), we find

$$T^{[s]}(\theta) = \frac{4\, n \cos\psi \cos\theta}{(\cos\theta + n\cos\psi)^2} \times \left(\frac{n\cos\varphi - \sqrt{1 - n^2\sin^2\varphi}}{n\cos\varphi + \sqrt{1 - n^2\sin^2\varphi}}\right)^2 \exp\left[i\,\phi_{\text{Snell}}\right] \quad (8)$$

and

$$T^{[p]}(\theta) = \frac{4\, n \cos\psi \cos\theta}{(n\cos\theta + \cos\psi)^2} \times \left(\frac{\cos\varphi - n\sqrt{1 - n^2\sin^2\varphi}}{\cos\varphi + n\sqrt{1 - n^2\sin^2\varphi}}\right)^2 \exp\left[i\,\phi_{\text{Snell}}\right], \quad (9)$$

where

$$\phi_{\text{Snell}} = k\left[\sqrt{2}\, n\cos\varphi\overline{AB} + (n\cos\psi - \cos\theta)\frac{\overline{AD}}{\sqrt{2}}\right].$$

For $n \sin\varphi < 1$, the outgoing beam,

$$E_{\text{out}}^{[s,p]}(y, z) = E_0\, e^{ik\,z}\int_{-\pi/2}^{+\pi/2} d\theta\, T^{[s,p]}(\theta) g(\theta - \theta_0) \times \exp\left[i(\theta - \theta_0)k\, y - i\,\frac{(\theta - \theta_0)^2}{2}k\, z\right], \quad (10)$$

is centered at

$$y_{\text{Snell}} = -\left[\frac{\partial\phi_{\text{Snell}}}{k\,\partial\theta}\right]_0 = \cos\theta_0\left[(\tan\psi_0 + 1)\overline{AB} + (\tan\psi_0 - \tan\theta_0)\frac{\overline{AD}}{\sqrt{2}}\right]. \quad (11)$$

This represents the well-known geometrical shift predicted by the Snell law in ray optics.

For $n \sin\varphi > 1$ an additional phase comes from the internal reflection coefficients in (8) and (9):

$$\left\{\phi_{\text{GH}}^{[s]}, \phi_{\text{GH}}^{[p]}\right\} = -4\left\{\arctan\left[\frac{\sqrt{n^2\sin^2\varphi - 1}}{n\cos\varphi}\right], \arctan\left[\frac{n\sqrt{n^2\sin^2\varphi - 1}}{\cos\varphi}\right]\right\} \quad (12)$$

and a new shift (the well known GH shift) must be considered. The numerical data for the propagation through BK7 ($n = 1.515$) and fused silica ($n = 1.457$) are plotted in figures 3 and 4. The data clearly show the amplification for incidence in the critical region, and they are in excellent agreement with the analytical prediction for incidence far from the critical angle,

$$\left\{y_{\text{GH}}^{[s]}, y_{\text{GH}}^{[p]}\right\} = -\left[\left\{\frac{\partial\phi_{\text{GH}}^{[s]}}{k\partial\theta}, \frac{\partial\phi_{\text{GH}}^{[p]}}{k\,\partial\theta}\right\}\right]_0 = \frac{4\cos\theta_0\sin\varphi_0}{k\cos\psi_0\sqrt{n^2\sin^2\varphi_0 - 1}} \times \left\{1, \frac{1}{n^2\sin^2\varphi_0 - \cos^2\varphi_0}\right\}, \quad (13)$$

where the w_0 dependence disappears [2, 4, 23, 24]. The plots of the GH shift for BK7 and fused silica clearly show an axial dependence. This axial dependence, which has been recently investigated and recognized as a possible source of angular deviations in the optical path predicted by the Snell law [37], must be seen in the optical weak measurement curves as well. Understanding how this axial dependence modifies the optical weak measurement curves in the critical region is one of the main objectives of our study.

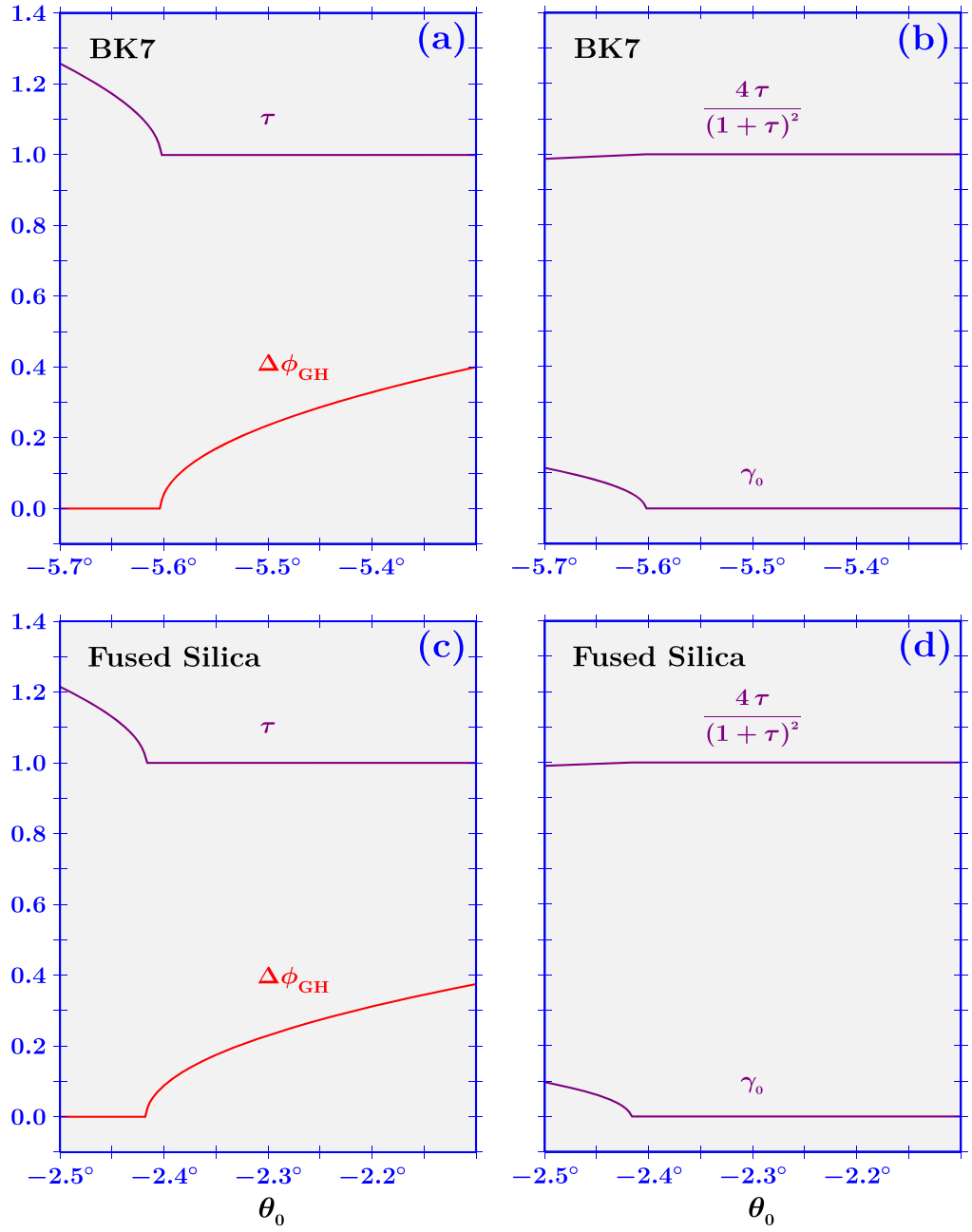

Figure 5. Angular dependence of τ, $\Delta\phi_{GH}$, and γ_0. The angular dependence of τ (ratio between the modulus of the amplitudes for s and p polarized light) and $\Delta\phi_{GH}$ (global phase difference between s and p polarized waves) are plotted in (a) for BK7 and (c) for fused silica blocks. The fact that in the critical region $4\,\tau/(1+\tau)^2$ is practically equal to 1 makes it is very useful to simplify the expression for the outgoing beam; see equation (19). The numerical data for γ_0 make it possible to calculate the second polarizer angle ($\beta_0 = 3\pi/4 + \gamma_0$), for which we find an outgoing beam with two identical maxima centered at $\pm w(z)$.

3. Weak measurements in optical experiments

On the basis of the results presented in the preceding section, we can approximate the s and p polarized outgoing beams as follows:

$$E_{out}^{[s,p]}(y,z) \approx \frac{E_0 e^{ik\,z}}{\sqrt{1+2\,i\frac{z}{k\,w_0^2}}}\left|T_0^{[s,p]}\right| \times \exp\left[-\frac{\left(y-y_{Snell}-y_{GH}^{[s,p]}\right)^2}{w_0^2+2\,i\,\frac{z}{k}} + i\left(\phi_{Snell,0}+\phi_{GH,0}^{[s,p]}\right)\right], \quad (14)$$

where for $y_{GH}^{[s,p]}$, which represents the only entry for which we do not have a full analytical expression, we must to use the numerical data plotted in figures 3 and 4.

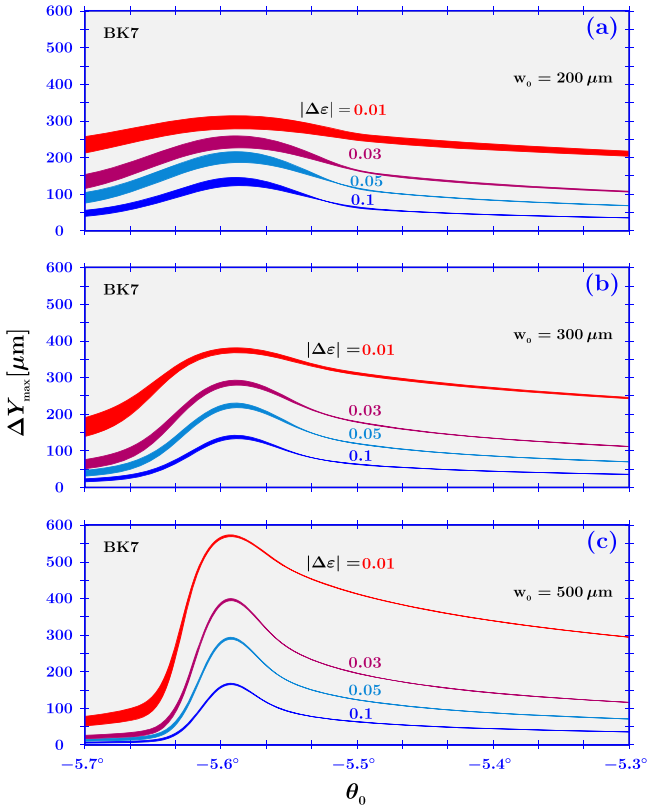

Figure 6. Optical weak measurements curves for BK7 blocks. The expected curves for the distance between the main peaks of the beams coming out from a BK7 dielectric block and passing through the second polarizer for two opposite rotations, $|\Delta\epsilon| = |\Delta\gamma|/\cos^2\gamma_0$, are plotted in the axial range 10 cm $\leqslant z \leqslant$ 15 cm for different beam waists, (a) $w_0 = 200\,\mu$m, (b) 300 μm, and (c) 500 μm. From the plots, it is clear that to improve the crossover frequency and to reduce the axial dependence, we have to work with $w_0 \geqslant 500\,\mu$m. Note that, also working with $w_0 = 500\,\mu$m, the curve amplification $1/|\Delta\epsilon|$, valid for incidence far from the critical region, is lost when the incidence angle approaches the critical angle.

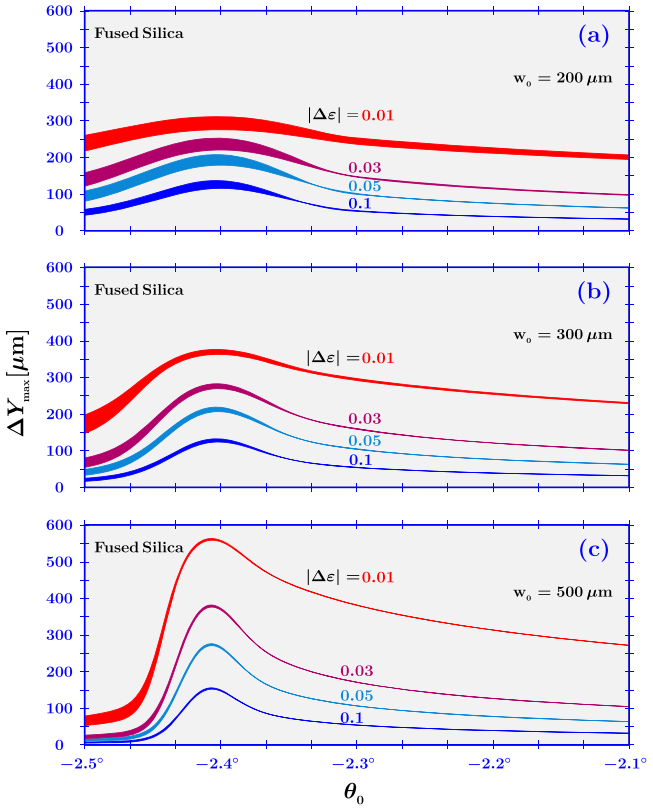

Figure 7. Optical weak measurement curves for fused silica blocks. The expected curves for the distance between the main peaks of the beams coming out from a fused silica dielectric block and passing through the second polarizer for two opposite rotations, $|\Delta\epsilon| = |\Delta\gamma|/\cos^2\gamma_0$, are plotted in the axial range 10 cm $\leqslant z \leqslant$ 15 cm for different beam waists, (a) $w_0 = 200\,\mu$m, (b) 300 μm, and (c) 500 μm. From the plots, it is clear that to improve the crossover frequency and to reduce the axial dependence, we have to work with $w_0 \geqslant 500\,\mu$m. Note that, also working with $w_0 = 500\,\mu$m, the curve amplification $1/|\Delta\epsilon|$, valid for incidence far from the critical region, is lost when the incidence angle approaches the critical angle.

The intensity of the outgoing beam coming out from the dielectric block and moving toward the analyzer ($z_{out} < z < z_A$ in figure 1) is given by

$$I_{out}\left(y, z_{out} < z < z_A\right) = \left|\sin\alpha\, E^{[s]}_{out}(y, z) + \cos\alpha E^{[p]}_{out}(y, z)\right|^2 \propto \left|\tau\tan\alpha\exp\left[-\left(\frac{y - y_{Snell} - y^{[s]}_{GH}}{w(z)}\right)^2 + i\,\Delta\phi_{GH}\right] + \exp\left[-\left(\frac{y - y_{Snell} - y^{[p]}_{GH}}{w(z)}\right)^2\right]\right|^2, \quad (15)$$

where $\tau = |\,T_0^{[s]}/\,T_0^{[p]}\,|$ and $\Delta\phi_{GH} = \phi^{[s]}_{GH,0} - \phi^{[p]}_{GH,0}$. The θ_0 dependence of τ and $\Delta\phi_{GH}$ is plotted in figures 5(a) (BK7) and (b) (fused silica). After removing the phase difference between the s and p polarized light by the analyzer located at $z = z_A$ and combining s and p polarization by the second polarizer located at $z = z_\beta$, the outgoing beam intensity becomes

$$I_{out}\left(Y, z > z_\beta\right) \propto \left|\tau\tan\alpha\tan\beta\exp\left[-\left(\frac{Y + \frac{\Delta y_{GH}}{2}}{w(z)}\right)^2\right] + \exp\left[-\left(\frac{Y - \frac{\Delta y_{GH}}{2}}{w(z)}\right)^2\right]\right|^2, \quad (16)$$

where

$$Y = y - y_{\text{Snell}} - \frac{y_{\text{GH}}^{[s]} + y_{\text{GH}}^{[p]}}{2} \quad \text{and} \quad \Delta y_{\text{GH}} = y_{\text{GH}}^{[p]} - y_{\text{GH}}^{[s]}.$$

Observing that

$$\tan\alpha \tan\beta = \frac{\epsilon - 1}{\epsilon + 1} \approx \frac{\epsilon_0 - 1}{\epsilon_0 + 1} + \frac{2}{\left(\epsilon_0 + 1\right)^2}\Delta\epsilon,$$

the choice of an appropriate rotation γ_0 makes it possible to fix the parameter $\epsilon_0 (= \tan\gamma_0)$ to

$$\epsilon_0 = \frac{\tau - 1}{1 + \tau} \quad \Rightarrow \quad \frac{\epsilon_0 - 1}{\epsilon_0 + 1} = -\frac{1}{\tau}. \tag{17}$$

The angular dependence of γ_0 is plotted in figures 5(b) (BK7) and (d) (fused silica) for incidence angles in the critical region. This choice enables rewriting of the outgoing intensity in terms of the parameters τ and $\Delta\epsilon$ as follows:

$$\begin{aligned} I_{\text{out}}(Y, \Delta\epsilon) &\propto \left| \left[\frac{(1+\tau)^2}{2\tau}\Delta\epsilon - 1 \right] \exp\left[-\left(\frac{Y + \frac{\Delta y_{\text{GH}}}{2}}{\text{w}(z)} \right)^2 \right] \right. \\ &\left. + \exp\left[-\left(\frac{Y - \frac{\Delta y_{\text{GH}}}{2}}{\text{w}(z)} \right)^2 \right] \right|^2 \\ &\approx \left\{ 2\left[\frac{(1+\tau)^2}{4\tau}\Delta\epsilon + \frac{\Delta y_{\text{GH}}}{\text{w}^2(z)} Y \right] \exp\left[-\frac{Y^2}{\text{w}^2(z)} \right] \right\}^2. \end{aligned} \tag{18}$$

Finally, noting that, in the critical region, $(1+\tau)^2 \approx 4\tau$ (see figures 5(b)–(d), we can get a further simplification of the outgoing beam intensity:

$$I_{\text{out}}(Y, \Delta\epsilon) \propto \left[\Delta\epsilon + \frac{\Delta y_{\text{GH}}}{\text{w}^2(z)} Y \right]^2 \exp\left[-\frac{2Y^2}{\text{w}^2(z)} \right]. \tag{19}$$

4. Behavior of peaks in the critical angle region

The starting point in optical weak measurement experiments is to set the angles of the first and second polarizers to

$$\left\{\alpha_0, \beta_0\right\} = \left\{ \frac{\pi}{4}, \frac{3\pi}{4} + \gamma_0 \right\}.$$

For this choice ($\Delta\epsilon = 0$) we find that the outgoing intensity,

$$I_{\text{out}}(Y, 0) \propto Y^2 \exp\left[-\frac{2Y^2}{\text{w}^2(z)} \right], \tag{20}$$

is a symmetric function with two peaks centered at $Y_{\text{max}}^{\pm} = \pm\text{w}(z)/\sqrt{2}$ and a minimum centered at $Y_{\text{min}} = 0$. By changing the angle of the second polarizer from β_0 to $\beta_0 + \Delta\gamma$, we break the symmetry. In terms of $\Delta\epsilon = \Delta\gamma/\cos^2\gamma_0$, we find

$$Y_{\text{min}}(\Delta\epsilon) = -\frac{\Delta\epsilon}{\Delta y_{\text{GH}}}\text{w}^2(z) \tag{21}$$

and

$$\begin{aligned} &Y_{\text{max}}^{\pm}(\Delta\epsilon) \\ &= \frac{-\Delta\epsilon \pm \sqrt{(\Delta\epsilon)^2 + 2\left[\Delta y_{\text{GH}}^2/\text{w}^2(z)\right]}}{2\Delta y_{\text{GH}}}\text{w}^2(z). \end{aligned} \tag{22}$$

It is clear that for positive $\Delta\epsilon$ (counterclockwise rotation $\Delta\gamma$ around γ_0), $Y_{\text{max}}^{+}(|\Delta\epsilon|)$ represents the position of the main peak of the outgoing beam. For negative $\Delta\epsilon$, the main peak is instead centered at $Y_{\text{max}}^{-}(-|\Delta\epsilon|)$. By using equation (22), the distance between these peaks is given by

$$\begin{aligned} \Delta Y_{\text{max}} &= Y_{\text{max}}^{+}(|\Delta\epsilon|) - Y_{\text{max}}^{-}(-|\Delta\epsilon|) \\ &= \frac{-|\Delta\epsilon| + \sqrt{|\Delta\epsilon|^2 + 2\left[\Delta y_{\text{GH}}^2/\text{w}^2(z)\right]}}{\Delta y_{\text{GH}}}\text{w}^2(z). \end{aligned} \tag{23}$$

In the region $0 \leqslant |\Delta\epsilon| \leqslant \Delta y_{\text{GH}}/\text{w}(z)$, we find

$$\sqrt{2}\,\text{w}(z) \leqslant \Delta Y_{\text{max}} \leqslant \left(\sqrt{3} - 1\right)\text{w}(z). \tag{24}$$

This clearly shows that by increasing the value of $|\Delta\epsilon|$, we reduce the distance between the peaks. For $|\Delta\epsilon| \gg \Delta y_{\text{GH}}/\text{w}(z)$,

$$\Delta Y_{\text{max}} \approx \Delta y_{\text{GH}}/|\Delta\epsilon|. \tag{25}$$

For incidence angles far from the critical region, because the GH shift is proportional to the wavelength of the laser beam, the condition

$$\frac{\Delta y_{\text{GH}}}{\text{w}(z)} \approx \frac{\lambda}{\text{w}(z)} \ll |\Delta\epsilon|$$

can be easily satisfied. Thus, far from the critical region, the experimental curves of ΔY_{max} reproduce the GH curves amplified by the factor $1/|\Delta\epsilon|$.

In the critical region, the frequency crossover and the axial dependence, shown in figures 3 (BK7) and 4 (fused silica), work against the validity of the constraint $|\Delta\epsilon| \gg \Delta y_{\text{GH}}/\text{w}(z)$. This means that in this region, the experimental curves of ΔY_{max} do not necessarily reproduce the GH curves. The expected experimental curves of the distance between peaks are plotted for different values of $|\Delta\epsilon|$ in figures 6 (bk7) 7 (fused silica). The plots confirm that, at critical incidence, the amplification does not reproduce the $1/|\Delta\epsilon|$ proportionality. The axial dependence is removed by increasing the beam waist w_0.

For experimental use, it is convenient to express the GH shift, Δy_{GH}, in terms of the experimental quantity ΔY_{max}. From

equation (23), we obtain

$$\Delta y_{\mathrm{GH}} = \frac{2\,|\Delta\epsilon|\,\mathrm{w}^2(z)}{2\,\mathrm{w}^2(z) - \Delta Y_{\mathrm{max}}^{\,2}}\,\Delta Y_{\mathrm{max}}. \tag{26}$$

The error in the GH shift is given by

$$\frac{\sigma\left(\Delta y_{\mathrm{GH}}\right)}{\Delta y_{\mathrm{GH}}} = \sqrt{\begin{array}{l}\left[\dfrac{\sigma(|\Delta\epsilon|)}{|\Delta\epsilon|}\right]^2 \\ \quad + \left[\dfrac{2\,\mathrm{w}^2(z) + \Delta Y_{\mathrm{max}}^{\,2}}{2\,\mathrm{w}^2(z) - \Delta Y_{\mathrm{max}}^{\,2}}\,\dfrac{\sigma\left(\Delta Y_{\mathrm{max}}\right)}{\Delta Y_{\mathrm{max}}}\right]^2 \\ \quad + \left\{\dfrac{2\,\Delta Y_{\mathrm{max}}^{\,2}}{2\,\mathrm{w}^2(z) - \Delta Y_{\mathrm{max}}^{\,2}}\,\dfrac{\sigma[\mathrm{w}(z)]}{\mathrm{w}(z)}\right\}^2\end{array}}.$$

Recalling that for $\Delta\epsilon = 0$, the distance between the peaks gives direct information about the beam waist, $\Delta Y_{\mathrm{max}} = \sqrt{2}\,\mathrm{w}(z)$, we can use

$$\sigma\left(\Delta Y_{\mathrm{max}}\right) = \sigma[\mathrm{w}(z)]$$

in the preceding error formula and obtain

$$\frac{\sigma\left(\Delta y_{\mathrm{GH}}\right)}{\Delta y_{\mathrm{GH}}} = \sqrt{\begin{array}{l}\left[\dfrac{\sigma(|\Delta\epsilon|)}{|\Delta\epsilon|}\right]^2 + \left[\dfrac{2\mathrm{w}^2(z) + \Delta Y_{\mathrm{max}}^{\,2}}{2\mathrm{w}^2(z) - \Delta Y_{\mathrm{max}}^{\,2}}\right]^2 \\ \quad \times\left\{1 + \left[\dfrac{2\Delta Y_{\mathrm{max}}^{\,3}\big/\mathrm{w}(z)}{2\mathrm{w}^2(z) + \Delta Y_{\mathrm{max}}^{\,2}}\right]^2\right\}\left[\dfrac{\sigma\left(\Delta Y_{\mathrm{max}}\right)}{\Delta Y_{\mathrm{max}}}\right]^2\end{array}}.$$

In the region $\mathrm{w}(z) \leqslant \Delta Y_{\mathrm{max}} \leqslant \sqrt{2}\,\mathrm{w}(z)$, we find

$$13 \leqslant \left[\frac{2\mathrm{w}^2(z) + \Delta Y_{\mathrm{max}}^{\,2}}{2\,\mathrm{w}^2(z) - \Delta Y_{\mathrm{max}}^{\,2}}\right]^2\left\{1 + \left[\frac{2\,\Delta Y_{\mathrm{max}}^{\,3}\big/\,\mathrm{w}(z)}{2\,\mathrm{w}^2(z) + \Delta Y_{\mathrm{max}}^{\,2}}\right]^2\right\} \leqslant \infty.$$

To avoid great standard deviations, we must work in the region $\Delta Y_{\mathrm{max}} \leqslant \mathrm{w}(z)$, where

$$\sqrt{\left[\frac{\sigma(|\Delta\epsilon|)}{|\Delta\epsilon|}\right]^2 + \left[\frac{\sigma\left(\Delta Y_{\mathrm{max}}\right)}{\Delta Y_{\mathrm{max}}}\right]^2} \leqslant \frac{\sigma\left(\Delta y_{\mathrm{GH}}\right)}{\Delta y_{\mathrm{GH}}} \leqslant \sqrt{\left[\frac{\sigma(|\Delta\epsilon|)}{|\Delta\epsilon|}\right]^2 + 13\left[\frac{\sigma\left(\Delta Y_{\mathrm{max}}\right)}{\Delta Y_{\mathrm{max}}}\right]^2}. \tag{27}$$

From the aforementioned condition on ΔY_{max}, by using equation (26) we obtain

$$|\Delta\epsilon| \geqslant , \frac{\Delta y_{\mathrm{GH}}}{2\mathrm{w}(z)}. \tag{28}$$

The choice of $|\Delta\epsilon_{\mathrm{min}}| = \Delta y_{\mathrm{GH}}/2\,\mathrm{w}(z)$ in the second polarizer thus is an additional experimental constraint to avoid great standard deviations.

5. Conclusions and outlook

The possibility of using the weak measurement of the electron spin component [31] in optics [28, 29] has recently stimulated an experiment [27] based on the interference between different polarizations, in which the GH shift curves are reproduced in the region of the validity of the standard analytic formula (13). Nevertheless, the analytical shift (13) diverges when the incidence angle approaches the critical angle. In a recent paper [23], this divergence was removed and an analytic formula, valid for $2z \ll k\mathrm{w}_0^2$, was proposed for the GH shift at the critical angle:

$$\left\{y_{\mathrm{GH}}^{[s]}, y_{\mathrm{GH}}^{[p]}\right\}_{\mathrm{cri}} \approx \frac{\sqrt{k\,\mathrm{w}(z)}}{k} \times \sqrt{2\sqrt{2\pi}\,\frac{\sqrt{2 - n^2 + 2\sqrt{n^2 - 1}}}{n^2 - 1 + \sqrt{n^2 - 1}}}\left\{1, n^2\right\}. \tag{29}$$

This closed formula, which is in excellent agreement with the numerical data plotted in figures 3(c) and 4(c), clearly shows the crossover frequency at the critical angle. The amplification $\sqrt{k\,\mathrm{w}(z)}$ at the critical angle suggested studying with more care the behavior of the peaks in the beam in optical weak measurements for incidence within the critical region. Indeed, in such a region, due to this amplification, the condition $|\Delta\epsilon| \gg \Delta y_{\mathrm{GH}}/\mathrm{w}(z)$ and the consequent proportionality among the experimental curves of the distance between peaks and the GH curves are no longer valid; see, for example, figures 6(c) and 7(c).

In our study, we have also found an axial dependence in optical weal measurements. This axial dependence can affect the experimental curves and, for small second polarizer rotations and small values of the beam waist, produces a practically flat region; see the plots in figures 6(a) and 7(a) for $|\Delta\epsilon| = 0.01$. To minimize the axial dependence, we have to work with a laser beam with $\mathrm{w}_0 \geqslant 500\,\mu$m. It is important to observe here that, also for $\mathrm{w}_0 = 500\,\mu$m, the curve amplification $1/|\Delta\epsilon|$ can be reproduced far from the critical region only.

In view of a possible experimental analysis of the study presented in this article, we have also estimated in which region we reach the better standard deviation for Δy_{GH} in the critical region. By using the second polarizer angle constraint, equation (28), and the analytical formula for the GH shift at the critical angle, equation (29), we find

$$|\Delta\epsilon| \geqslant \sqrt{\sqrt{\frac{\pi}{2}}\frac{\sqrt{2-n^2+2\sqrt{n^2-1}}}{n^2-1+\sqrt{n^2-1}}}\frac{n^2-1}{\sqrt{k\,\mathrm{w}(z)}}. \qquad (30)$$

This implies that for laser beams with $w_0 = 500\,\mu$m and a camera at $z \leqslant 50$ cm, $|\Delta\epsilon_{min}| \approx 0.015$ for both BK7 and fused silica dielectric blocks.

We conclude this work by observing that our analysis does not take into account cumulative dissipations and imperfections in the dielectric prism (such as the misalignment of its surfaces) and beam reshaping caused by interference. A phenomenological way to include misalignment effects is given in reference [37]. An interesting discussion of the origin of negative and positive lateral shifts in a dielectric slab is investigated in reference [38] from the viewpoint of the interference between multiple light beams.

Acknowledgments

The authors thank the Capes (M P A) and CNPq (S D L and G G M) for financial support. One of the authors (S D L) is greatly indebted to S A Carvalho for interesting comments and stimulating discussions. Finally, the authors thank the referees for their useful observations and suggestions.

References

[1] Goos F and Hänchen H 1947 Ein neuer und fundamenta ler versuch zur totalreflexion *Ann. Phys.* **436** 333–46
[2] Artmann K 1948 Berechnung der seitenversetzung des totalreflektierten strahles *Ann. Phys.* **437** 87–102
[3] Fragstein C v 1949 zur Seitenversetzung des totalreflektierten lichtstrahles *Ann. Phys.* **439** 271–8
[4] McGuirk M and Carniglia C K 1977 An angular spectrum representation approach to the Goos–Hänchen shift *J. Opt. Soc. Am.* **67** 103–7
[5] Cowan J J and Anicin B 1977 Longitudinal and transverse displacements of a bounded microwave beam at total internal reflection *J. Opt. Soc. Am.* **67** 1307–14
[6] Yasumoto K and Oishi Y 1983 A new evaluation of the Goos-Hänchen shift and associated time delay *J. Appl. Phys.* **54** 2170–6
[7] Puri A, Pattanayak D N and Birman J L 1983 Resonance effects on total internal reflection and lateral (Goos-Hänchen) beam displacement at the interface between nonlocal and local dielectric *Phys. Rev.* B **28** 5877–86
[8] Birman J L, Pattanayak D N and Puri A 1983 Prediction of a resonance-enhanced laser-beam displacement at total internal reflection in semiconductors *Phys. Rev. Lett.* **50** 1664–7
[9] Seshadri S R 1988 Goos-Hänchen beam shift at total internal reflection *J. Opt. Soc. Am.* A **5** 583–5
[10] Emile O, Galstyan T, Le Floch A and Bretenaker F 1995 Measurement of the nonlinear Goos-Hänchen effect for gaussian optical beams *Phys. Rev. Lett.* **75** 1511–3
[11] Baida F I, Labeke D V and Vigoureux J M 2000 Numerical study of the displacement of a three-dimensional gaussian beam transmitted at total internal reflection. Near-field applications *J. Opt. Soc. Am.* A **17** 858–66
[12] Broe J and Keller O 2002 Quantum-well enhancement of the Goos-Hänchen shift for p-polarized beams in a two-prism configuration *J. Opt. Soc. Am.* A **19** 1212–22
[13] Born M and Wolf E 1999 *Principles of Optics* (Cambridge: Cambridge University Press)
[14] Saleh B E A and Teich M C 2007 *Fundamentals of Photonics,* (New Jersey: Wiley & Sons)
[15] Liu X and Yang Q 2010 Total internal reflection of a pulsed light beam with consideration of Goos-Hänchen effect *J. Opt. Soc. Am.* B **27** 2190–4
[16] Prajapati C and Ranganathan D 2012 Goos-Hänchen and Imbert-Federov shifts for Hermite-Gauss beams *J. Opt. Soc. Am.* A **29** 1377–82
[17] Aiello A 2012 Goos-Hänchen and Imbert-Federov shifts: a novel perspective *New J. Phys.* **14** 013058–12
[18] Wan Y, Zheng Z, Kong W, Zhao X, Liu Y, Bian Y and Liu J 2012 Nearly three orders of magnitude enhancement of Goos-Hänchen shift by exciting Bloch surface wave *Opt. Exp.* **20** 8998–9003
[19] Bliokh K Y and Aiello A 2013 Goos-Hänchen and Imbert-Fedorov beam shifts: an overview *J. Opt.* **15** 014001–16
[20] Prajapati C and Ranganathan D 2013 The effect of spectral width on Goos-Hänchen and Imbert-Federov shifts *J. Opt.* **15** 025703–10
[21] Götte J B, Shinohara S and Hentschel M 2013 Are Fresnel filtering and the angular Goos-Hänchen shift the same? *J. Opt.* **15** 014009–8
[22] Araújo M P, Carvalho S A and De Leo S 2014 The asymmetric Goos-Hänchen effect *J. Opt.* **16** 015702–7
[23] Aráujo M P, Carvalho S A and De Leo S 2013 The frequency crossover for the Goos-Hänchen shift *J. Mod. Opt.* **60** 1772–80
[24] Horowitz B R and Tamir T 1971 Lateral displacement of a light beam at a dielectric interface *J. Opt. Soc. Am.* **61** 586–94
[25] Wigner E 1955 Lower limit for the energy derivative of the scattering phase shift *Phys. Rev.* **98** 145–7
[26] Bleistein N and Handelsman R 1975 *Asymptotic Expansions of Integrals* (New York: Dover)
[27] Jayaswal G, Mistura G and Merano M 2013 Weak measurement of the Goos-Hänchen shift *Opt. Lett.* **38** 1232
[28] Duck I M, Stevenson P M and Sudarshan E C G 1989 The sense in which a 'weak measurement' of a spin 1/2 particle's spin component yields a value 100 *Phys. Rev.* D **40** 2112–7
[29] Dennis M R and Götte J B 2012 The analogy between optical beam shifts and quantum weak measurements *New J. Phys.* **14** 073013–13
[30] Götte J B and Dennis M R 2012 Generalized shifts and weak values for polarization components of reflected light beams *New J. Phys.* **14** 073016–20
[31] Aharonov Y, Albert D Z and Vaidman L 1988 How the result of a measurement of a component of the spin of a spin 1/2 particle can turn out to be 100 *Phys. Rev. Lett.* **60** 1351–4
[32] De Leo S and Rotelli P 2008 Localized beams and dielectric barriers *J. Opt.* A **10** 115001–5
[33] De Leo S and Rotelli P 2011 Laser interacting with a dielectric block *Eur. Phys. J.* D **61** 481–8

[34] De Leo S and Rotelli P 2011 Resonant laser tunneling *Eur. Phys. J.* D **65** 563–70
[35] Carvalho S A and De Leo S 2013 Light transmission thorugh a triangular air gap *J. Mod. Opt.* **60** 437–43
[36] Carvalho S A and De Leo S 2013 Resonance, multiple diffusion and critical tunneling for gaussian lasers *Eur. Phys. J.* D **67** 168–11
[37] Araújo M P, Carvalho S A and De Leo S 2014 Maximal breaking of symmetry at critical angle and closed-form expression for angular deviations of the Snell law *Phys. Rev.* A **90** 033844–11
[38] Chen X and Li C F 2009 Negative and positive lateral shifts: a result of beam reshaping caused by interference *J. Opt.* A **11** 085004–6